AIAA JOURNAL
Vol. 34, No. 1, January 1996

# Identification of Impact Force and Location Using Distributed Sensors

Keeyoung Choi* and Fu-Kuo Chang†
*Stanford University, Stanford, California 94305-4035*

**An impact load identification method using distributed built-in sensors for detecting foreign object impact is proposed. The identification system consists of a system model and a response comparator. The system model characterizes the dynamic response of the structure subject to a known impact force. The comparator compares the measured sensor outputs with the estimated measurements from the model and predicts the location and force history of the impact. The method has been developed for beams containing distributed piezoelectric sensors. The identification system was tested using simulated conditions. For all of the cases considered, the estimation errors fell well within the prespecified limit.**

## I. Introduction

DAMAGE due to an external impact is a major concern in the design of aerospace structures. For instance, low-velocity impact can cause extensive delaminations inside composite structures that could severely degrade the load-carrying capability of the structures. In many cases, however, it is not easy to identify this damage by visual inspection. For structures susceptible to impact, routine nondestructive testing must be performed over the entire surface. A few examples of the traditional methods are coin tapping,[1,2] x ray,[3,4] and ultrasound.[5–7] Because the location of impact is unknown, all of these are quite time consuming, costly, and require the structural system to be out ot service. Therefore, a system that can automatically detect the occurrence of impact and estimate the amount of impact energy, as well as the location, would be very helpful in maintaining the structures at reduced cost.

The impact load identification problem has two characteristics that make it difficult to solve. First, it is an inverse problem. Compared with a direct dynamics problem whose goal is to find the system response for the given system model and driving force, the load identification problem tries to find the input force for a given system response. Second, it is a nonlinear problem. Think of a case involving a structure excited by a force whose time history is known. The output will be different depending on the location of where the force is applied. Thus, it can be deduced that the system equations that define the relation between input (external force) and output (measurement) are functions of an unknown parameter (loading point). Since the load parameters, the location and history, are to be found based on a system model whose parameter (the location) is unknown, the identification process is nonlinear.

One of the oldest inverse problems is finding the source of an earthquake using arrival-time data at several different stations.[8] This kind of approach has been applied to structural impact identification, too. Mannas and Joshi[9] tried to estimate the impact point using lag time for a composite plate with piezoelectric patches used as sensors. The lag time was determined by looking for the signal to rise to a certain level. For noisy, dispersive waves, this lag time is very difficult to find, and the accuracy of the method may degrade. For a beam, Whiston[10] and Jordan and Whiston[11] used the arrival-time difference between the maximum- and minimum-frequency components to calculate a preliminary estimation of the location of the wave origin. Starting from this initial estimation, a further refinement process proceeded to reconstruct the impact history iteratively so that the force would not have a negative portion. This approach can be applied only to an impact involving an outward normal contact force. With this method, it is also necessary to find a systematic way to proceed with the iteration in the refinement procedure when the estimated location is not so close to the impact point. Michaels and Pao[12] developed a method that determined an oblique dynamic force using wave motion measurement. In this case, the location of the force was known, and the time history and orientation of the force were identified using measured displacements at known locations.

Doyle[13–15] published papers on a method for determining the location and magnitude of an impact force using the phase difference of the signals measured at two different sensors straddling the impact point. The method was verified with an experiment using a long aluminum beam. Estimating reliable phase information for noisy signals, however, requires great effort and usually requires human interference.

Most of the propagating-wave approaches have relied on models in the frequency domain. On the other hand, time-domain models are widely used for standing-wave approaches. Busby and Trujillo[16] showed that the input force history can be reconstructed by solving a dynamic inverse problem, and Hollandsworth and Busby[17] verified this experimentally. In the experiment, the load was applied at a known position and accelerometers were used as sensors. For an unknown loading point, D'Cruz et al.[18,19] formulated a nonlinear inverse problem and tried to find the location and magnitude of the external force. The force, however, was not general but confined to a sinusoidal function whose amplitude and phase are the only parameters to be found.

This paper presents a new load identification method based on distributed sensor measurements. The method could be easily automated and implemented in a structural monitoring system. It will be demonstrated for identifying impact load and location in beams containing distributed piezoelectric sensors.

## II. Load Identification System

Figure 1 is a schematic drawing of a conceptual load identification system that can estimate the location and time history of an impact load using the measured signals from the sensors built into the structure. The load identification system consists of two parts: a structure model and a response comparator (inverse problem solver). The structure model characterizes the relation between the input load and the sensor output. The response comparator compares the measured sensor output with the model prediction and updates the parameters: the location and force history. The structural system considered here was a beam with piezoelectric sensors mounted on the back surface (Fig. 2). For given sensor measurements, it was intended that the location and history of the impact on the beam be predicted. The following assumptions were made for the system model.

1) The changes in the system characteristics before and after the impact are ignorable.

Received Dec. 5, 1994; revision received June 15, 1995; accepted for publication Aug. 15, 1995. 

*Department of Aeronautics and Astronautics; also Aerospace Engineer, Advanced Rotorcraft Technology, Mountain View, CA 94043. Member AIAA.

†Associate Professor, Department of Aeronautics and Astronautics. Member AIAA.

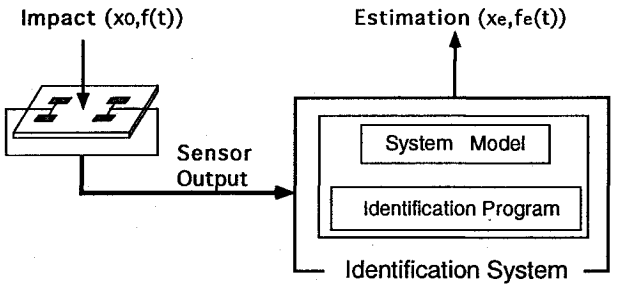


**Fig. 1 Schematic drawing of the proposed impact load identification system.**

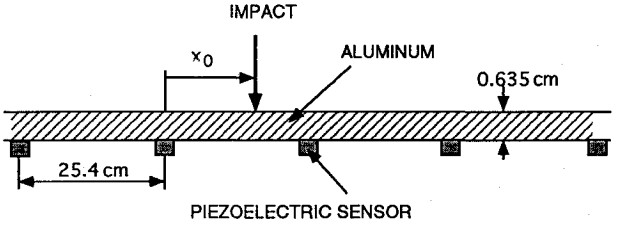


**Fig. 2 Beam with piezoelectric sensors and subjected to an impact load.**

2) The force is a perfect point force.
3) Structural damping is negligible.
4) The structure is at rest before an external load is applied.

### A. System Model

*1. Equations of Motion*

As an extreme case, if a long beam with high damping is subject to an impact that lasts for a short time period, the phenomena are localized. Generally speaking, if the localized phenomena are the main interest, the motion of the beam is described with a propagating-wave model and the boundary effects can be ignored. On the other hand, if the boundaries are close to the impact point and global phenomena are more important, a standing-wave model is more efficient to represent the system behavior. It has been shown that the solutions of these two models converge on each other as the number of modes and number of reflection waves increase.[20] The proposed identification system is general and can be applied to both models. For the sake of simplicity, this paper will deal with the propagating-wave model only. People who are interested in the standing-wave model may read Ref. 20.

Without considering shear and rotary inertia effects, the response of the beam is governed by the following Bernoulli–Euler beam equation:

$$\rho A\frac{\partial^2 w}{\partial t^2}+EI\frac{\partial^4 w}{\partial x^4}=f(x,t) \tag{1}$$

where $\rho$ is the density and $A$ and $EI$ are the area and the moment of inertia of a cross section, respectively. Here, $w$ is the deflection, and $f(x,t)$ is the applied force. Because this partial differential equation is not an efficient form to be used in the identification process, it is necessary to convert it into a simpler ordinary differential equation. Because this paper concentrates on the identification of impact force, a propagating-wave model will be derived. For the derivation of a standing-wave model, see Choi[20] and Tse et al.[21]

Applying discrete Fourier transformations with respect to the spatial variable $x$ on both sides yields a component equation

$$\frac{d^2\bar{w}_n}{dt^2}+\frac{EI}{\rho A}k_n^4\bar{w}_n=\frac{1}{\rho A\Delta_x}f(t) \tag{2}$$

where

$$\bar{w}_n=\bar{w}_n(k_n,t)=\sum_{n=0}^{n_s}w(x,t)e^{-ik_nx}$$

The number of data points is $n_s+1$. $\Delta_x$ is analogous to the sampling period in the time domain.

This is a second-order ordinary differential equation with respect to time and can be integrated easily if $f(t)$ is given. Once $\bar{w}$ is known, the original signal can be recovered using the inverse Fourier transformation

$$w(x,t)=\sum_{n=0}^{n_s}\bar{w}(k_n,t)e^{ik_nx} \tag{3}$$

Equation (2) can be converted to a set of first-order differential equations. We can write the $n$th component as

$$\frac{d}{dt}\begin{bmatrix}\bar{w}_n\\ \dot{\bar{w}}_n\end{bmatrix}=\begin{bmatrix}0 & 1\\ -\dfrac{EI}{\rho A}k_n^4 & 0\end{bmatrix}\begin{bmatrix}\bar{w}_n\\ \dot{\bar{w}}_n\end{bmatrix}+\begin{bmatrix}0\\ \dfrac{1}{\rho A\Delta_x}\end{bmatrix}f(t) \tag{4}$$

Let

$$\bar{\boldsymbol{w}}\triangleq[\bar{w}_0\quad\bar{w}_1\quad\cdots\quad\bar{w}_{n_s}]^T$$

where each component satisfies Eq. (4). Collecting these component equations generates the system equation in state-space form as

$$\dot{z}=\frac{d}{dt}\begin{bmatrix}\bar{\boldsymbol{w}}\\ \dot{\bar{\boldsymbol{w}}}\end{bmatrix}=\begin{bmatrix}\boldsymbol{0} & \boldsymbol{I}\\ \boldsymbol{K} & \boldsymbol{0}\end{bmatrix}\begin{bmatrix}\bar{\boldsymbol{w}}\\ \dot{\bar{\boldsymbol{w}}}\end{bmatrix}+\begin{bmatrix}\boldsymbol{0}\\ \boldsymbol{b}\end{bmatrix}f(t)$$

$$\triangleq \boldsymbol{A}\boldsymbol{z}+\boldsymbol{B}f(t) \tag{5}$$

where $\boldsymbol{I}$ is the identity matrix of size $n_s+1$. Here, $\boldsymbol{b}$ is defined as

$$\boldsymbol{b}=\frac{1}{\Delta_x}\left[\frac{1}{\rho A}\cdots\frac{1}{\rho A}\right]^T$$

$\boldsymbol{K}$ is a diagonal matrix of

$$\boldsymbol{K}=-(EI/\rho A)\ \mathrm{diag}\left(k_0^4,k_1^4,\ldots,k_{ns}^4\right)$$

The displacement at $x=x_j$ is represented with the following observation equation:

$$y(x_j,t)=(1/2n_s)[e^{ik_0x_j}\quad e^{ik_1x_j}\quad\cdots\quad e^{ik_{n_s}x_j}]\bar{\boldsymbol{w}} \tag{6}$$

Since $y$ is a real, even function, it can be calculated with real functions only:

$$y(x_j,t)$$
$$=(1/2n_s)\left[\cos(k_0x_j)\quad 2\cos(k_1x_j)\quad\cdots\quad 2\cos\left(k_{n_s}x_j\right)\right]\bar{\boldsymbol{w}}$$
$$\triangleq \boldsymbol{C}\bar{\boldsymbol{w}} \tag{7}$$

*2. Piezoelectric Sensors*

Because of the coupling between mechanical and electrical quantities, piezoelectric materials can be used either as sensors or actuators. This study uses piezoelectric materials as sensors. Detailed derivation of the governing equation for piezoelectric materials can be found in various sources.[22–24] This section will derive the relation between the piezoelectric sensor output and the states of the structure system. For the sake of simplicity, we ignore the structual effect of the piezoelectric material.

The observation equation for a piezoelectric sensor can be derived by assuming that the voltage output of the sensor is proportional to the integral of strain over the piezoelectric material. Let us start from the displacement equation [Eq. (7)]. The displacement is given in terms of the state variables as

$$w(x,t)=\boldsymbol{C}(x)\boldsymbol{z} \tag{8}$$

Now, the strain on the top surface of the beam is represented as

$$\epsilon=\frac{h}{2}\frac{\partial^2 w}{\partial x^2}=\frac{h}{2}\left(\frac{\partial^2\boldsymbol{C}(x)}{\partial x^2}\right)\boldsymbol{z} \tag{9}$$

where $h$ is the thickness of the beam. Since the voltage output of a piezoelectric sensor is proportional to the integral of strain over piezoelectric material, we can write it as

$$\begin{aligned} v_j &= a\int_{V_{pj}} \epsilon \, dV \\ &= \left(a\frac{h}{2}\int_{V_{pj}} \frac{\partial^2 \boldsymbol{C}}{\partial x^2} dV\right) z \\ &\triangleq \boldsymbol{C}_v z \end{aligned} \tag{10}$$

where $V_{pj}$ is the volume of the $j$th piezoelectric patch and $a$ is a material dependent proportional constant.

*3. Equation of Motion in Discrete Time Domain*

Because most data processing, including a data acquisition, is now done in digital form, a discrete-time version of the system equation is necessary. Many current textbooks on digital control explain this process.[25] The system model in the continuous-time domain is given as

$$\dot{z}(t) = \boldsymbol{A}z(t) + \boldsymbol{B}f(t) \tag{11}$$

$$y(t) = \boldsymbol{C}z(t) \tag{12}$$

The discrete version of the system equation is

$$\begin{aligned} z(n+1) &= \begin{bmatrix} \phi_{11} & \phi_{12} \\ \phi_{21} & \phi_{22} \end{bmatrix} z(n) + \begin{bmatrix} \gamma_1 \\ \gamma_2 \end{bmatrix} f(n) \\ &\triangleq \boldsymbol{\Phi} z(n) + \boldsymbol{\Gamma} f(n) \end{aligned} \tag{13}$$

where $\phi_{ij}$ are diagonal matrices and, thus, $\boldsymbol{\Phi}$ is a block diagonal matrix. The observation equation is given as

$$y(n) = \boldsymbol{C}z(k) \tag{14}$$

where $y(n)$ is a measurement at time $t = T_s$. $T_s$ is the sampling period.

The system matrices of the two representations are related as

$$\boldsymbol{\Phi} = \exp(\boldsymbol{A}T_s) \tag{15}$$

$$\boldsymbol{\Gamma} = \int_0^{T_s} \exp(\boldsymbol{A}t)\, dt\, \boldsymbol{B} \tag{16}$$

Note that the observation matrix $\boldsymbol{C}$ is not affected by the digitization process.

**B. Response Comparator**

For an infinite beam, a coordinate system centered on the wave origin (loading point) was used and the observation matrix was a function of the distances between the sensors and the wave origin (Fig. 2). If the wave origin is known with respect to any one sensor, then the other sensor locations are automatically determined because the distances among sensors are given. Let $x_0$ be the actual distance between a designated sensor and the forcing point and $x_e$ its estimate. The goal of the identification scheme is to find the location parameter $x_e$ and force history $f(n)$ so that the model prediction matches the measured response as closely as possible.

Let us write the discrete-time system equation as [Eqs. (13 and 14)]

$$\begin{aligned} z_{n+1} &= \boldsymbol{\Phi} z_n + \boldsymbol{\Gamma} f_n \\ y_j(n) &= \boldsymbol{C}(x_j) z_n, \qquad n = 0, \ldots, (N-1) \end{aligned} \tag{17}$$

where $N$ is the total number of sampling points and $y_j(n)$ is the measured quantity (displacement, strain, etc.) at the sensor located at a distance of $x_j$ from the wave origin at time $t = nT_s$.

The problem can be formulated as a nonlinear least-squares problem

$$\begin{aligned} \min_{x_e, f} J &= \frac{1}{2}[z(0) - z_0]^T S_0 [z(0) - z_0] + \frac{1}{2}\sum_{n=0}^{N-1} f_n Q f_n \\ &+ \frac{1}{2}\sum_{n=0}^{N} \nu_n^T R \nu_n + \frac{1}{2}[z(N) - z_N]^T S_f [z(N) - z_N] \end{aligned} \tag{18}$$

where $z_0$ and $z_N$ are user-supplied guesses of initial and final states. Because this study assumes that the system is at rest before the impact, $z_0$ is set to zero. Here, $\nu$ is the difference between the measured outputs $y_m$ and the model predictions $y_e$ that contains both the effects of measurement noise and error due to incorrect estimation of the location or history of the external force, i.e.,

$$\nu_n = y_{e,n}(x_e, f) - y_{m,n} \tag{19}$$

$Q$ is weighting for the input force and $\boldsymbol{R}$ for the states. $S_0$ and $S_f$ are weighting matrices for the initial and final conditions, respectively. For the reason given earlier, $S_0$ is set very high. On the other hand, since the final condition is unpredictable (unless the structural damping is significantly large), $S_f$ is set to zero.

The minimization is subject to the constraint equations [Eq. (17)]. The performance index is modified to accommodate these constraints using Lagrange multipliers $\lambda$:

$$\bar{J} = J + \sum_{n=0}^{N-1} \lambda^T [\Phi z_n + \Gamma f_n - z_{n+1}] \tag{20}$$

Minimizing $\bar{J}$ is equivalent to minimizing $J$ subject to the constraints of Eq. (17). Idan and Bryson[26] used the smoothing algorithm successfully to find system parameters of a helicopter using flight test data. This identification algorithm closely follows that of Ref. 26.

Taking a variation on this augmented performance index gives

$$\delta \bar{J} = \sum_{n=0}^{N} \frac{\partial \bar{J}}{\partial z_n}\delta z_n + \sum_{n=0}^{N-1} \frac{\partial \bar{J}}{\partial f_n}\delta f_n + \frac{\partial \bar{J}}{\partial x_e}\delta x_e \tag{21}$$

Without the third term, the problem is an ordinary linear two-point boundary-value problem (LTPBVP) that can be solved using a well-known smoothing algorithm.[26,27]

The third derivative term depends on the functional relation between the system matrix and the parameter ($x_e$). It is calculated as

$$\frac{\partial \bar{J}}{\partial x_e} = \sum_{n=0}^{N-1} \lambda_{n+1}^T \frac{\partial \Gamma(x_e)}{\partial x_e} f_n - \sum_{n=1}^{N} \nu_n^T R \frac{\partial C(x_e)}{\partial x_e} z_n \tag{22}$$

Since $\nu_n$ are calculated in the smoothing process, the calculation can be done quickly. This is one of the great benefits of this smoothing technique in the sense that the solution of the LTPBVP gives the information necessary to update the location $x_e$.

The identification process has two loops. In the outer loop, the location of the load is estimated. The inner loop is a linear least-square fitting process that predicts the force history based on the estimated location transferred from the outer loop. Solving this LTPBVP belongs to this inner loop. In the outer loop, the parameter $x_e$ (location of the force measured from a sensor) is updated using a quasi-Newton procedure to minimize $\bar{J}$:

$$x_{e,\text{new}} = x_{e,\text{old}} - \bar{J}_{xx}^{-1} \bar{J}_{x_e} \tag{23}$$

The inverse of the Hessian matrix $\bar{J}_{xx}^{-1}$ is estimated numerically from successive values of the gradient vector $\bar{J}_{x_e}$ using a rank-two update procedure.[28,29] If the Hessian matrix is set to the identity matrix, then the method is equivalent to the steepest descent method; this is used for the first update in the outer loop. Figure 3 depicts the identification process for a certain initial guess of the location $x_{e,0}$. Since the problem is nonlinear with respect to the loading point, it is likely that multiple local minima exist. A nonlinear function optimizer is needed to handle this problem. Expert systems and genetic

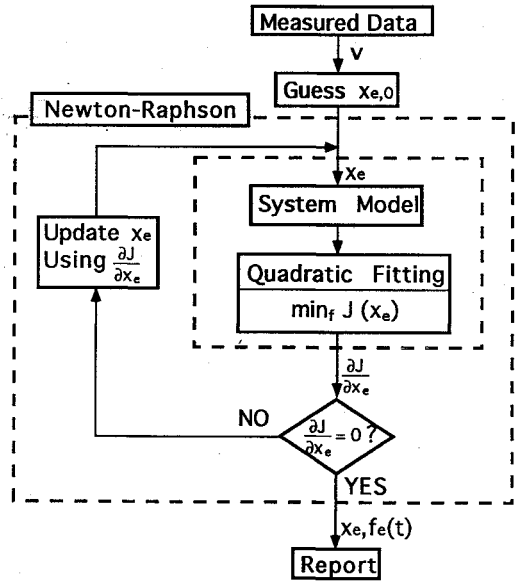


**Fig. 3 Load identification process.**

algorithms are examples of such nonlinear techniques. This study uses the simplest one, multiple initial guesses. A local minimum is found for each initial guess following the procedure shown in Fig. 3. Among the resultant local minima, the smallest one is taken as the global minimum.

## III. Results

### A. Model Verification

The propagating-wave model derived in a preceding section will be verified. Doyle[13] published a paper on identifying dynamic contact force. He measured strain histories at various locations of an aluminum beam hit by a swinging steel ball. The contact force estimation from Ref. 13 by Doyle drove the simulation. The strain histories at the contact point and 4.45 cm away from the contact point were calculated with the previously derived model (Fig. 4). The good agreement between the measurement and simulation prediction verifies the modeling.

### B. Example of the Identification Procedure

To verify the comparator developed in the preceding section, numerical simulation results based on the system model were generated. To add reality to the verification procedure, random white noises were added to the nominal responses, and the results were used to simulate the actual sensor measurements. For the given simulated sensor measurements, the load identifier was used to estimate the location and history of the impact. A schematic description of the simulation procedure is given in Fig. 5. The goal is to find $x_e$ and $f_e$ so that the predicted system response matches best with the measured sensor output. The two system models are not necessarily the same. Because the purpose of the current study is to develop an identification system, however, the same model was used in both places, i.e., it was assumed that the system model used in the identification is exact.

The model used in this paper appears in Fig. 2. The piezoelectric sensors are 0.5 cm long and separated by 25.4 cm from each other. In the identification process, four sensors were used. The impact point was assumed to be within the two outmost sensors. In practical application, this should not pose any serious problem since it is easy to isolate a certain region that includes the impact point by looking at the wave-propagation shape. Structural damping makes the work even easier. Ideally, two sensors are enough to find the location and load history for a beam problem.[20] Because of the measurement noise, however, more sensors will increase the accuracy of the result. The aluminum beam is 0.635 cm thick.

Figure 6 shows the simulated sensor output of the structure subject to a triangular shape force of maximum magnitude 1000 N and duration 0.3 ms. The plot shows a nominal signal with computer-generated noise added. This noisy signal is used in the identification

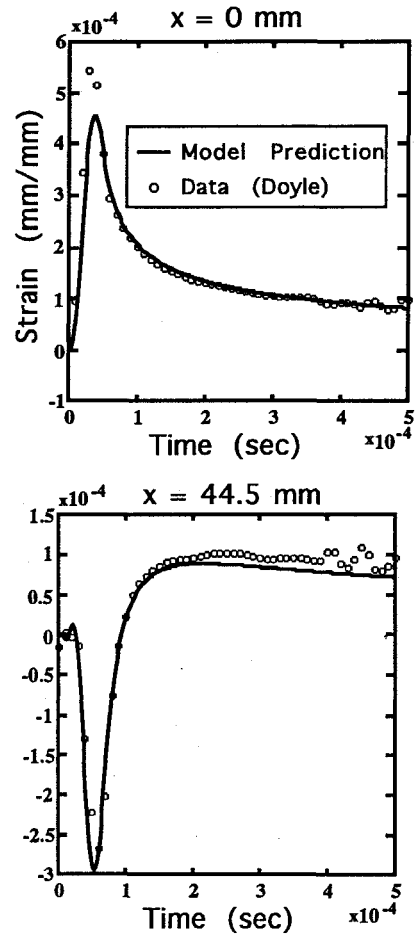


**Fig. 4 Strain history: measured and calculated.**

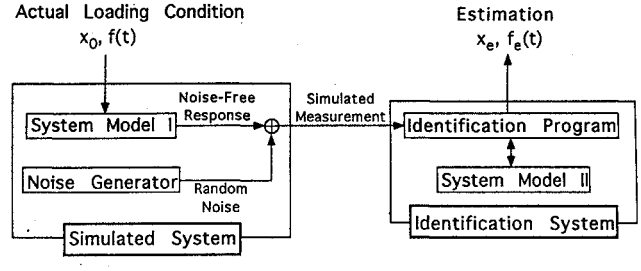


**Fig. 5 Schematic description of the simulation procedures.**

procedure, whereas the nominal output is unknown to the identification procedure and used only for results verification purposes. The distance between the leftmost sensor and the loading point was 27.18 cm. All four sensors were distributed evenly with a separation of 25.4 cm.

For various guesses of the impact locations $x_e$, the smoothing problems were solved and the performance indices were calculated. Figure 7 plots the resultant performance indices as a function of $x_e$. We see that several stationary points exist, and the global minimum corresponds to the actual forcing point. For this example, points separated by 12.7 cm were selected as initial guess points. From each of these initial guesses, the local minimum was sought using the gradient information ($dJ/dx_e$) that is calculated by solving the quadratic fitting problem. The global-searching process appears in Fig. 8. The actual distance between the impact point and the leftmost sensor was 27.18 cm, whereas the estimation was 27.31 cm. Figure 9 shows the estimated force history along with the actual load.

For a problem like this, 100 wave components were used, and it typically took about 30 min to complete the computation on a workstation. At the time when the authors developed this scheme, they did not pay particular attention to the optimization of the computation time. The identification scheme was programmed in MATLAB

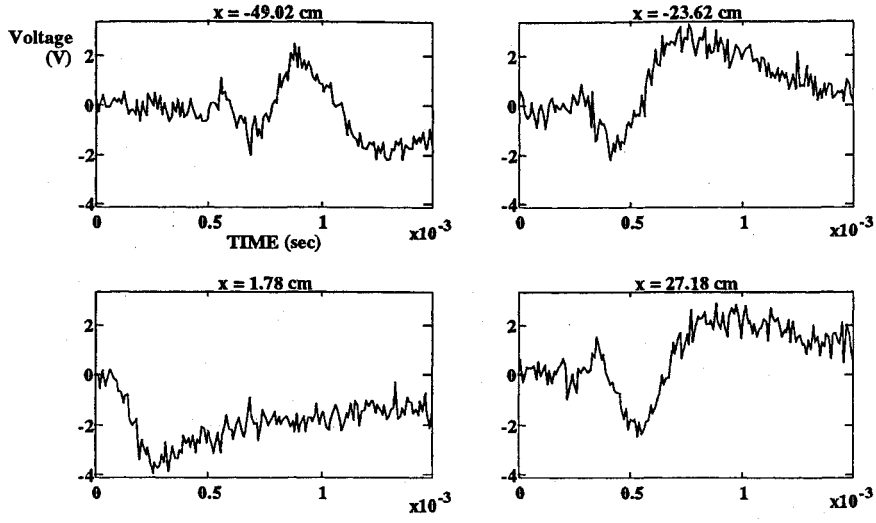


Fig. 6 Simulated sensor outputs with added random white noise.

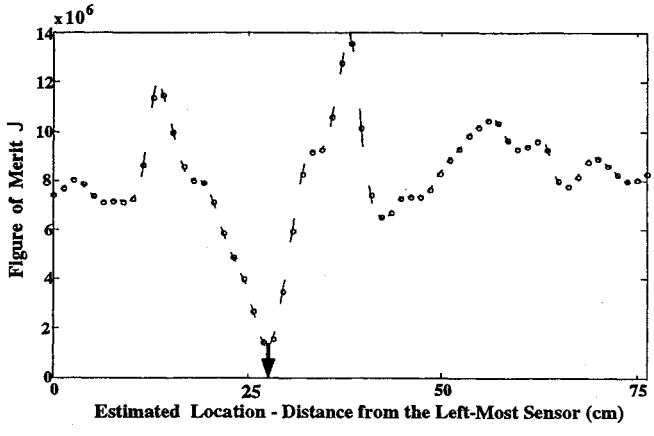


Fig. 7 Distribution of the figure of merit $J$ as a function of the estimated impact location.

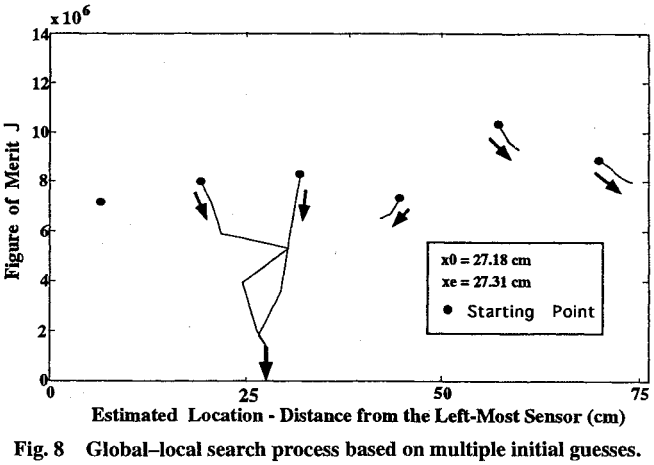


Fig. 8 Global–local search process based on multiple initial guesses.

scripts. If it is programmed in compile languages such as C or Fortran, the computation time could be reduced significantly.

### C. Verification Using Simulation Results

The identification process was applied to more cases to check the stability of the system. First, to show that the comparator works for general loading histories, a case with an external force that has both positive and negative parts was generated. Figure 10 shows the result. The specific external load shape was the sine function of a period. The estimated impact position was 35.48 cm compared with the actual position of 35.56 cm. Despite the fluctuation, the estimated load history matched the actual one quite closely.

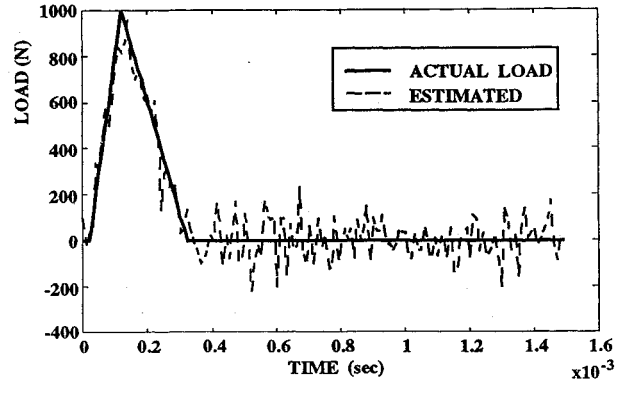


Fig. 9 Comparison between the predicted and the actual impact load history.

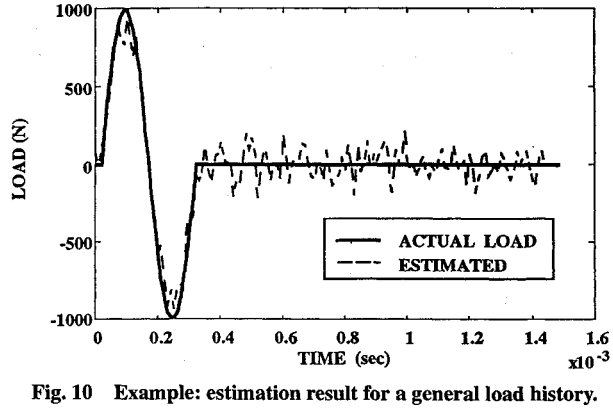


Fig. 10 Example: estimation result for a general load history.

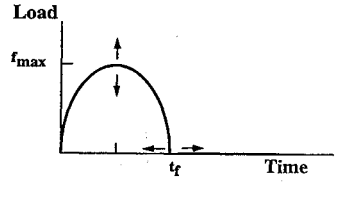


Fig. 11 General load history.

To test the reliability further, 100 cases were simulated. In each case, the parameters of the loading history and the forcing point were varied randomly around the nominal values used in the previous example. A typical load history appears in Fig. 11. Since the identification program was not aware of the shape of the actual load history, this half-sine pulse shape was a legitimate type as a random force. Also, a half-sine shape is believed to closely approximate real

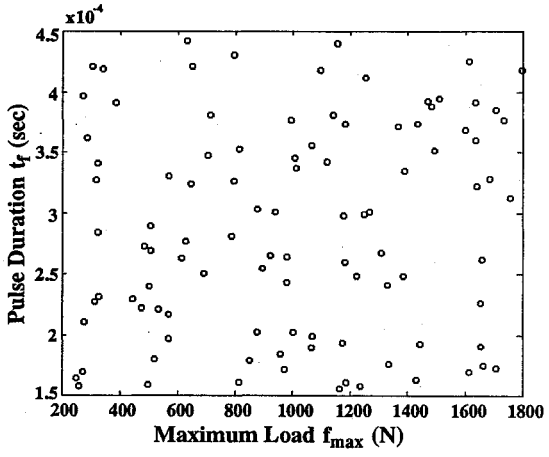


Fig. 12 Variation in the simulation conditions.

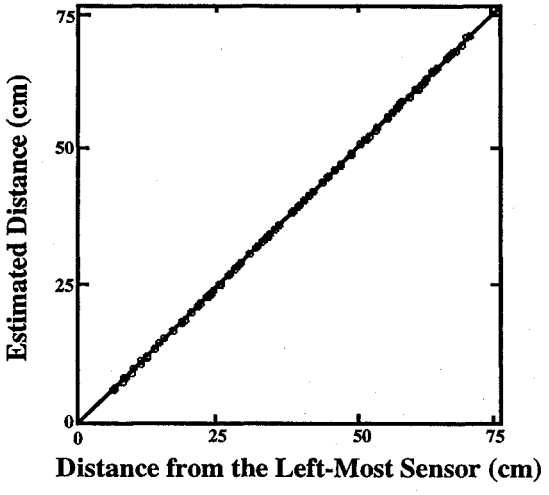


Fig. 13 Identification results: loading point estimation.

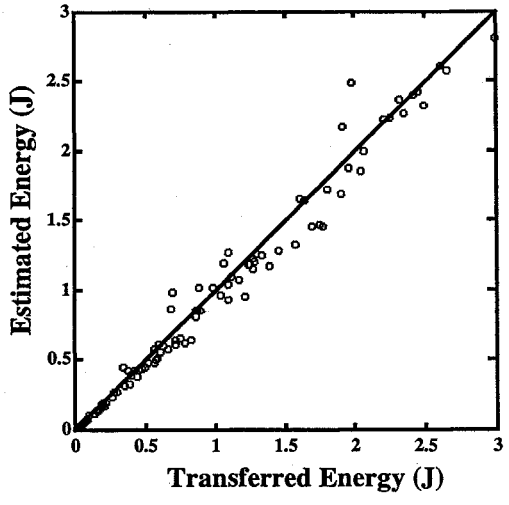


Fig. 14 Identification results: energy transferred.

contact force histories. The maximum magnitude and duration were variables. Figure 12 depicts the loading conditions used in the verification process. The results of the loading point estimation were plotted in Fig. 13. The fact that most of the data points fell along the 45-deg lines verifies the system stability.

To show the load history estimation, impact energy was used. Going back to the very first part of the problem, the main goal of this study is to develop a method that can give information in predicting damage caused by an external force. Instead of using the whole history of the load, the total energy transferred to the structure is more useful and convenient to predict the scope of the damage. Once the force history is estimated, the energy can be calculated with the following formula:

$$\text{energy} = \int f(t)\,dw \approx \sum_{i=0}^{N-1} \frac{[f(n+1)+f(n)]}{2}[w_0(n+1)-w_0(n)] \quad (24)$$

where $w_0$ is the displacement at the forcing point and can be calculated using the estimated location and force history. Figure 14 shows the transferred energy estimation. As with the loading point estimation, most of the data are scattered close to the 45-deg line.

## IV. Concluding Remarks

An impact load identification method has been proposed for estimating the location and history of an impact force in structures. The method has been successfully applied to beams containing distributed piezoelectric sensors. Using a realistic numerical simulation, the algorithm was proved to be stable. It is possible to extend the method to more complicated structures. In this case, some modifications of the comparator are expected, whereas the system model will have to be developed based on the type of structures considered.

## Acknowledgments

Partial support of this research by a grant from the AFOSR is gratefully appreciated. K. Choi would like to thank A. E. Bryson of Stanford University for his valuable suggestions and discussions during the course of the investigation.

## References

[1]Cawley, P., "The Impedance Method of Non-Destructive Inspection," *NDT International*, Vol. 17, No. 2, 1984, pp. 59–65.

[2]Cawley, P., "Low Frequency NDT Techniques for the Detection of Disbonds and Delaminations," *British Journal of Non-Destructive Testing*, Vol. 32, Sept. 1990, pp. 454–461.

[3]Smith, B., "Failure Analysis Procedures," *Engineered Materials Handbook*, Vol. 1, ASM International, 1987, pp. 770–773.

[4]Henneke, E., II, "Destructive and Nondestructive Tests," *Engineered Materials Handbook*, Vol. 1, ASM International, 1987, pp. 774–778.

[5]Teagle, P., "The Quality Control and Non-Destructive Evaluation of Composite Materials and Components," *Design with Advanced Composite Materials*, Springer–Verlag, Berlin, 1991, pp. 221–242.

[6]Dewen, P. N., and Cawley, P., "An Ultrasonic Scanning Technique for the Quantitative Determination of the Cohesive Properties of Adhesive Joints," *Review of Progress in Quantitative NDE*, edited by D. Thompson and D. Chimenti, Vol. 11, Plenum, New York, 1992, pp. 1253–1260.

[7]Tom, P., and Cawley, P., "The Detection of a Weak Adhesive/Adherend Interface in Bonded Joints by Ultrasonic Reflection Measurements," *Review of Progress in Quantitative NDE*, edited by D. Thompson and D. Chimenti, Vol. 11, Plenum, New York, 1992, pp. 1261–1266.

[8]Aki, K., and Richards, P. G., *Quantitative Seismology—Theory and Methods*, Vols. 1, 2, W. H. Freeman, San Fransisco, CA, 1980.

[9]Mannas, J. R., and Joshi, S. P., "Study of Smart Sensing Elements in a Dynamic Stress Field," *Smart Sensing, Processing, and Instrumentation*, Vol. 1918, Society of Photo-Optical Instrumentation Engineers, Washington, DC, 1993, pp. 264–273.

[10]Whiston, G., "Remote Impact Analysis by Use of Propagated Acceleration Signals, I: Theoretical Methods," *Journal of Sound and Vibration*, Vol. 97, No. 1, 1984, pp. 35–51.

[11]Jordan, R., and Whiston, G., "Remote Impact Analysis by Use of Propagated Acceleration Signals, II: Comparison between Theory and Experiment," *Journal of Sound and Vibration*, Vol. 97, No. 1, 1984, pp. 53–63.

[12]Michaels, J., and Pao, Y.-H., "Determination of Dynamic Forces from Wave Motion Measurements," *Journal of Applied Mechanics*, Vol. 53, March 1986, pp. 61–68.

[13]Doyle, J. F., "Further Developments in Determining the Dynamic Contact Law," *Experimental Mechanics*, Vol. 24, Dec. 1984, pp. 265–270.

[14]Doyle, J. F., "An Experimental Method for Determining the Location and Time of Initiation of an Unknown Dispersing Pulse," *Experimental Mechanics*, Vol. 27, Sept. 1987, pp. 229–233.

[15]Doyle, J. F., "Determining the Contact Force During the Transverse Impact of Plates," *Experimental Mechanics*, Vol. 24, March 1987, pp. 68–72.

[16]Busby, H. R., and Trujillo, D. M., "Solution of an Inverse Dynamics Problem Using an Eigenvalue Reduction Technique," *Computers and Structures*, Vol. 25, No. 1, 1987, pp. 109–117.

[17]Hollandsworth, P. E., and Busby, H. R., "Impact Force Identification Using the General Inverse Technique," *International Journal of Impact Engineering*, Vol. 8, No. 4, 1989, pp. 315–322.

[18]D'Cruz, J., Crisp, J. D., and Ryall, T. G., "Determining a Force Acting on a Plate—An Inverse Problem," *AIAA Journal*, Vol. 29, No. 3, 1991, pp. 464–470.

[19]D'Cruz, J., Crisp, J., and Ryall, T., "Determining a Dynamic Force on a Plate—A Non-Linear Inverse Problem," *Australian Vibration and Noise Conference*, Inst. of Engineers, Australia, 1990, pp. 218–221.

[20]Choi, K., "An Impact Load Identification Using Distributed Sensor Measurements," Ph.D. Thesis, Dept. of Aeronautics and Astronautics, Stanford Univ., Stanford, CA, Dec. 1993.

[21]Tse, F. S., Morse, I. E., and Hinkle, R. T., *Mechanical Vibrations—Theory and Applications*, 2nd ed., Allyn and Bacon, Boston, MA, 1978, pp. 262–284.

[22]Hagood, N. W., Chung, W. H., and von Flotow, A., "Modelling of Piezoelectric Actuator Dynamics for Active Structural Control," *31st Structures, Structural Dynamics, and Materials Conference*, AIAA, Washington, DC, 1990, pp. 2242–2256.

[23]Auld, B. A., *Acoustic Fields and Waves in Solids*, 2nd ed., Kreiger, Malabar, FL, 1990, pp. 265–356.

[24]Tzou, H. S., and Tseng, C. I., "Distributed Piezoelectric Sensor/Actuator Design for Dynamic Measurement/Control of Distributed Parameter System: A Piezoelectric Finite Element Approach," *Journal of Sound and Vibration*, Vol. 138, No. 1, 1990, pp. 17–34.

[25]Franklin, G. F., Powell, J. D., and Workman, M. L., *Digital Control of Dynamic Systems*, 2nd ed., Addison–Wesley, Reading, MA, 1990, pp. 46–56.

[26]Idan, M., and Bryson, A. E., Jr., "Parameter Identification of Linear Systems Based on Smoothing," *Journal of Guidance, Control, and Dynamics*, Vol. 15, No. 4, 1992, pp. 901–911.

[27]Bryson, A. E., Jr., "Optimal Estimation and Control," Lecture notes for E207C, Stanford Univ., Stanford, CA, 1992.

[28]Luenberger, D., *Linear and Nonlinear Programming*, 2nd ed., Addison–Wesley, Reading, MA, 1984, pp. 260–279.

[29]Cuthbert, T., Jr., *Optimization Using Personal Computers with Application to Electrical Networks*, Wiley, New York, 1987.